1 Cellular and molecular characterization of multiplex autism in human induced pluripotent

2 stem cell-derived neurons

- 3 Emily M.A. Lewis¹*, Kesavan Meganathan¹*, Dustin Baldridge², Paul Gontarz¹, Bo Zhang¹, Azad
- 4 Bonni³, John N. Constantino⁴ and Kristen L. Kroll^{1**}
- 5 *Contributed equally
- 6 **Corresponding Author
- 7 Departments of ¹Developmental Biology, ²Pediatrics, ³Neuroscience, and ⁴Psychiatry
- 8 Washington University School of Medicine, St. Louis, MO 63110
- 9 Emily M. A. Lewis e.lewis@wustl.edu
- 10 Kesavan Meganathan meganathank@wustl.edu
- 11 Dustin Baldridge dbaldri@wustl.edu
- 12 Paul Gontarz pgontarz@wustl.edu
- 13 Bo Zhang bzhang29@wustl.edu
- 14 Azad Bonni bonni@wustl.edu
- 15 John N. Constantino constantino@wustl.edu
- 16 <u>Corresponding Author:</u>
- 17 Kristen L. Kroll kkroll@wustl.edu
- 18 Phone 314-362-7045
- 19 Fax 314-362-7058

20 Abstract

Background: Autism spectrum disorder (ASD) is a neurodevelopmental disorder with pronounced heritability in the general population. This is largely attributable to effects of polygenic susceptibility, with inherited liability exhibiting distinct sex differences in phenotypic expression. Attempts to model ASD in human cellular systems have principally involved rare *de novo* mutations associated with ASD phenocopies. However, by definition, these models are not representative of polygenic liability, which accounts for the vast share of population-attributable risk.

Methods: Here, we performed what is, to our knowledge, the first attempt to model multiplex 28 29 autism using patient-derived induced pluripotent stem cells (iPSCs) in a family manifesting 30 incremental degrees of phenotypic expression of inherited liability (absent, intermediate, severe). The family members share an inherited variant of unknown significance in GPD2, a 31 gene that was previously associated with developmental disability but here is insufficient by 32 33 itself to cause ASD. iPSCs from three first-degree relatives and an unrelated control were differentiated into both cortical excitatory (cExN) and cortical inhibitory (cIN) neurons, and 34 cellular phenotyping and transcriptomic analysis were conducted. 35

Results: cExN neurospheres from the two affected individuals were reduced in size, compared 36 37 to those derived from unaffected related and unrelated individuals. This reduction was, at least in part, due to increased apoptosis of cells from affected individuals upon initiation of cExN 38 39 neural induction. Likewise, cIN neural progenitor cells from affected individuals exhibited 40 increased apoptosis, compared to both unaffected individuals. Transcriptomic analysis of both cExN and cIN neural progenitor cells revealed distinct molecular signatures associated with 41 42 affectation, including misregulation of suites of genes associated with neural development, 43 neuronal function, and behavior, as well as altered expression of ASD risk-associated genes.

Conclusions: We have provided evidence of morphological, physiological, and transcriptomic signatures of polygenic liability to ASD from an analysis of cellular models derived from a multiplex autism family. ASD is commonly inherited on the basis of additive genetic liability. Therefore, identifying convergent cellular and molecular phenotypes resulting from polygenic and monogenic susceptibility may provide a critical bridge for determining which of the disparate effects of rare highly deleterious mutations might also apply to common autistic syndromes. **Keywords:** Multiplex autism, iPSC modeling, neurodevelopment, cortical excitatory neurons, cortical inhibitory neurons, transcriptomics, gene networks.

64 Background

Autism spectrum disorder (ASD) is a neurodevelopmental disorder with a complex and poorly 65 66 understood etiology (1-3). Behavioral and imaging studies have been valuable for defining 67 deficits in affected individuals and characterizing alterations at the level of the brain. However, we are extremely limited in our ability to acquire or experimentally manipulate human brain 68 tissue from living patients or post-mortem brain slices. This has hampered efforts to study 69 70 cellular and molecular abnormalities that accompany ASD, both during and after fetal and post-71 natal development. Notably, both the relative integrity of brain structures in affected individuals 72 and the diversity of ASD genetics suggest that convergent mechanisms that contribute to affectation in ASD may operate at the level of the cell (3, 4). These may be identifiable in 73 74 experimental models derived from affected individuals. In particular, ASD appears to frequently 75 involve abnormal development and/or function of two major classes of neurons in the cerebral 76 cortex, glutamatergic excitatory projection neurons (cExNs) and GABAergic inhibitory 77 interneurons (cINs) (3, 5, 6). In vitro differentiation-based models of these neuronal cell types 78 can identify cellular and molecular deficits associated with ASD, and provide a tractable platform 79 to screen for pharmacologic agents that can rescue these deficits.

In recent years, such cellular models of ASD have been generated either by deriving 80 81 induced pluripotent stem cell lines (iPSCs) from affected individuals or by using CRISPR/Cas9-82 based gene editing to engineer ASD-associated mutations into wild type PSCs (7-19). Most of these studies have focused on syndromic forms of ASD, or on monogenic, de novo cases, 83 84 where causality is attributed to mutation of a single ASD-linked gene (10, 11, 13-16). These 85 forms of ASD are attractive for cellular modeling, as they streamline study design and reduce many potential confounding variables. Other studies have included individuals with an unknown 86 87 genetic cause of ASD, but with subject selection based upon a shared phenotypic characteristic, 88 such as macrocephaly (18-20). Together, these models have been informative, revealing both

cellular and molecular alterations associated with affectation. These include shared and model-89 90 specific disruptions of gene expression in ASD-derived neurons, frequently involving altered expression of genes in key developmental signaling pathways, and genes that control cellular 91 92 proliferation and growth (7, 8, 13-20). In addition, differences were observed in neural precursor 93 cell (NPC) proliferation and differentiation (9, 19), neurogenesis, (9, 11, 18, 20), synaptogenesis (8, 10, 17, 18), or functional neuronal activity (7-9, 11, 16, 17). Altered expression of ASD 94 95 genes, in which a mutation is linked to ASD causation or risk, is also frequently observed (7, 8, 13-16, 18-20). 96

97 These cellular modeling studies have revealed potential contributors to affectation and, in some cases, have identified targets amenable to pharmacological rescue in vitro (10, 18). 98 99 However, they do not encompass the range of contributors to ASD burden in the general 100 population: no single gene mutation accounts for more than 1% of overall ASD cases with 101 predicted monogenic causality (21), while the majority of genetic risk appears to be polygenic or idiopathic (2, 22-28). Polygenic ASD risk can involve both common and rare variation in protein-102 coding and non-coding regions of the genome, which may act in a combinatorial manner (2, 27, 103 104 29, 30). Furthermore, ASD exhibits pronounced heritability in families (estimated at 50-90%) (31)), none of which can be accounted for by *de novo* (germline) events. Even within each 105 106 multiplex ASD family, there is often a considerable range in the extent of affectation among individuals, and in most multiplex autism families, a single causative gene mutation usually 107 108 cannot be identified (31).

While ASD burden in the general population predominantly involves polygenic or idiopathic risk, heritability, and variable affectation (2, 21, 27, 29-31), these genetically complex forms of the disorder have been largely neglected in cellular modeling studies. Therefore, we deemed it important to determine whether cellular modeling of these complex but prevalent forms of ASD could also reveal affectation-related deficits. To test this, we focused on a

114 multiplex ASD family with variable affectation among family members. We generated iPSC lines 115 from three first degree relatives (a male and a female with differing degrees of affectation and their unaffected mother) as well as an unrelated unaffected female. We used these lines to 116 117 perform differentiation into both cExN and cIN neural progenitors and/or neurons. Models from 118 the affected individuals exhibited compromised cellular responses to differentiation cues and had disrupted gene expression profiles. This included altered expression of many ASD genes, 119 120 genes with roles related to behavior, cognition, and learning, and genes involved in nervous 121 system development and function, including cell adhesion molecules and ion channels.

This is, to our knowledge, the first cellular modeling study of multiplex ASD, including graded affectation among family members. We demonstrated that even genetically complex forms of ASD have discernable cellular and molecular abnormalities that track with affectation, some of which overlap those identified in prior modeling of syndromic, monogenic, and *de novo* forms of ASD. Therefore, this novel study design highlights the potential for cellular modeling to identify convergent hallmarks across the broad diversity and genetic complexity of pathways to affectation.

129 Methods

130 Phenotyping of the Multiplex Family

The nuclear family consisted of working professional non-consanguineous parents, whose first born child was a daughter with DSM-5 Autism Spectrum Disorder (ASD), Level I (requiring support, meeting DSM-5 criteria for Asperger Syndrome) who was very high functioning and ultimately attended college, followed by a pair of monozygotic twin boys with ASD, Level III one more fluently verbal than the other but both severely impaired and requiring very substantial support (see below)—followed by a third son with very subtle autistic traits and predominantly affected by Attention Deficit Hyperactivity Disorder which improved substantially with stimulant medication treatment. Trio Exome sequencing (ES) of one of the twins and his parents revealed a variant of unknown significance (VUS) in *GPD2*, which was inherited by all of the children from the mother, who is of above average intelligence with no dysmorphism and no history of developmental problems. All pregnancies were uncomplicated, except for the post-natal hospital course of the twins.

The daughter was born at term with no complications or dysmorphia. Her language and 143 motor development were typical and she was able to read at an early age. By age five she was 144 reading at a fifth-grade level. She has been described as talented in writing and drawing. 145 146 According to her parents, she exhibited social oddities from an early age, mainly in communication, and has somewhat intense/restricted interests in fantasy games. She has 147 148 strong language abilities, and currently attends a four-year college, but at times uses odd 149 phrases and the rhythm of her speech includes irregular pauses. She has described feeling 150 alienated and "different", and was the victim of bullying in middle school, with few close friends. In late adolescence, she developed major depressive disorder with moderate severity, which 151 152 brought her to first psychiatric contact. She is cognizant of some degree of social awkwardness, 153 which leads to feelings of anxiety and self-consciousness. The social anxiety inhibits her from activities such as eating in the cafeteria and pursuing job opportunities for which she is 154 otherwise well-qualified. She has a history of becoming emotionally dysregulated and 155 156 overwhelmed in times of stress, which has led to self-injurious behaviors. She has had ongoing struggles with depressive decompensation and suicidal ideation. She has above average 157 158 intelligence but has struggled academically in college due to depression and anxiety. She is 159 medically healthy with the exception of supraventricular tachycardia secondary to 160 atrioventricular node reentry, which was treated with ablation and resulted in subsequent 161 normalization of her electrocardiogram.

The twin boys were born at 35 weeks, had breathing problems at birth, and spent ten 162 163 days in the newborn intensive care unit. Neither child has any dysmorphic features or congenital 164 medical abnormalities, and brain imaging studies were negative. Likewise, neither child has a 165 history of confirmed seizures, however, there are concerns for possible absence epilepsy. There 166 is no history of abnormal neurological examination or macro-/microcephaly. Development of both siblings was delayed, but neither had appreciable regression. The more severely affected 167 168 twin (designated as the affected proband, AP, and from whom the incuced pluripotent stem cell 169 (iPSC) model of severe ASD affectation was acquired) began to exhibit delays in development 170 by nine months of age. He was speaking single words at 14 months and was ultimately 171 diagnosed with autism at 3.5 years old. Research confirmation of the diagnosis was obtained 172 using the Autism Diagnostic Observation Schedule. Compared to his twin brother, he has had 173 more perseverative interests on odd objects. Psychological testing at the age of nine revealed an IQ of 65 using the Leiter International Performance Scale. Now in late adolescence, he has 174 the ability to engage in reciprocal and meaningful verbal exchanges, although his language is 175 176 often echolalic and repetitive. He is socially motivated and develops superficial friendships with 177 peers. Functionally, he is able to complete most self-care, dress himself, prepare food and feed 178 himself, and count money. He participates in a vocational program at school and is able to complete rudimentary tasks assigned to him. His monozygotic twin was also diagnosed with 179 180 ASD at 3.5 years old and is less severely affected, but still requires significant support. Selected clinical characteristics of the family members studied are summarized in Table 1. 181

182 Genotyping of the Multiplex Family

Trio ES was performed by GeneDx for the unaffected mother (UM), the AP, and the unaffected father. Briefly, sequencing was performed on an Illumina platform and reads were aligned to human genome build GRCh37/hg19 and analyzed using Xome Analyzer, as described (32). Mutation-specific testing was also performed by GeneDx on the intermediate phenotype sister (IS) and the third trait-affected brother (TB) to confirm presence of the identified *GPD2* variant in
these individuals.

189 iPSC generation

iPSC lines were generated by the Genome Engineering and iPSC Center at Washington University. Briefly, renal epithelial cells were isolated and cultured from fresh urine samples and were reprogrammed using a CytoTune-iPS 2.0 Sendai Reprogramming kit (Thermo Fisher Scientific), following the manufacturer's instructions. iPSC clones were then picked, expanded, and characterized for pluripotency by immunocytochemistry (ICC) and RT-qPCR. At least three clonal iPSC lines were derived for each subject and two different clones were used for experimentation.

197 **iPSC maintenance and differentiation**

198 iPSC lines were grown under feeder-free conditions on Matrigel (Corning) in mTeSR1 (STEMCELL Technologies). cExN and cIN differentiation of iPSCs was performed using 199 previously described protocols (33). Briefly, for cExN differentiation, iPSCs were dissociated to 200 201 single cells with Accutase (Life Technologies) and 40,000 cells were seeded in V-bottom 96-well non-adherent plates (Corning). Plates were spun at 200xg for five minutes to generate embryoid 202 203 bodies (EBs) and were incubated in 5% CO₂ at 37°C in cExN differentiation medium with 10µM Y-27632 (Tocris Biosciences). cExN differentiation medium components include Neurobasal-A 204 205 (Life Technologies), 1X B-27 supplement (without Vitamin A) (Life Technologies), 10µM SB-206 431542 (Tocris Biosciences), 100nM LDN-193189 (Tocris Biosciences). On day four of 207 differentiation, EBs were transferred from V-bottom plates to Poly-L-Ornithine- (20µg/ml) and laminin- (10µg/ml) coated plates. Media (without Y-27632) was replenished every other day, 208 209 and on day 12 Neural Rosette Selection reagent (STEMCELL Technologies) was used to select 210 neural progenitor cells (NPCs) from within neural rosettes, per the manufacturer's instructions.

cExN NPCs were grown as a monolayer using cExN differentiation media for up to 15 211 212 passages. cIN differentiation media contained the same components as cExN differentiation media, while also including 1µM Purmorphamine (Calbiochem) and 2µM XAV-939 (Tocris 213 214 Biosciences). EBs were generated as described for cExNs. At day four of differentiation, the 215 EBs were transferred to non-adherent plates and were placed on an orbital shaker (80 rpm) in 216 an incubator with 5% CO₂ at 37°C. The media was replenished every other day and, at day ten, 217 EBs were transferred to Matrigel- and laminin- (5µg/ml) coated plates. Y-27632 was included in media until day eight of differentiation. On day 12 of differentiation, NPCs were dissociated with 218 219 Accutase and maintained as a monolayer for up to 15 passages. For both cIN and cExN NPC growth analysis, an equal number of cells were seeded on Matrigel- and laminin- (5µg/ml) 220 coated plates and total cells were counted four days later when the cells reached 70-80% 221 222 confluence.

For differentiation of cExN NPCs into neurons for maturation, 40,000 cells per well were 223 224 seeded in V-bottom 96-well non-adherent plates. Plates were spun at 200xg for five minutes 225 and incubated in 5% CO₂ at 37°C in maturation medium with Y-27632. Maturation medium 226 components include Neurobasal-A, 1X B-27 supplement (without Vitamin A), 200µM cAMP (Sigma), 200µM Ascorbic acid (Sigma), and 20ng BDNF (Tocris Biosciences). After two days, 227 EBs were transferred to Matrigel- and laminin- (5µg/ml) coated plates and media was 228 229 replenished every other day (without Y-27632). On day 12 of neuronal differentiation and 230 maturation, cells were dissociated with Accutase and seeded in an eight-well chamber for ICC.

For neurosphere size measurement analysis, p-values: *P<0.05, **P<0.01, ***P<0.001 were determined by a two-tailed Student's t-test.

233 Sanger Sequencing

DNA was isolated from cell lines using the PureLink Genomic DNA Kit (Invitrogen). Primers 234 235 were designed to amplify a 248 base pair region of GPD2 flanking the identified point mutation AAGCAGCAGACTGCATTTCA, 236 (forward primer: primer: reverse 237 CACCATGGCACACACTTACC). Sanger sequencing was performed on this PCR amplified 238 fragment using either the forward or reverse primer. CodonCode Aligner software was used to analyze sequencing results. 239

240 Immunocytochemistry (ICC) and Immunoblotting

For ICC, cells were plated on eight-well chamber slides coated with Matrigel and laminin (5 241 µg/mL). After one day, cells were washed once with PBS without calcium and magnesium (PBS 242 - Ca²⁺/Mg²⁺) and fixed in 4% Paraformaldehyde for 20 minutes, followed by washing with PBS + 243 Ca²⁺/Mg²⁺. Cells were blocked with blocking buffer (10% donkey serum, 1% BSA, and 0.1% 244 TritonX-100 in PBS + Ca²⁺/Mg²⁺) for at least one hour and incubated with primary antibodies 245 overnight (Additional file 1: Table S1) in antibody dilution buffer (1% donkey serum, 1% BSA, 246 and 0.1% TritonX-100 in PBS +Ca²⁺/Mg²⁺). After overnight incubation, cells were washed three 247 times with wash buffer (0.1% Triton X-100 in PBS + Ca^{2+}/Mq^{2+}). Cells were incubated with 248 corresponding secondary antibodies (Additional file 1: Table S1), along with DAPI (1mg/mL; 249 ThermoFisher Scientific), diluted in antibody dilution buffer for one hour. Following secondary 250 antibody incubation, cells were washed twice with wash buffer and once with PBS + Ca^{2+}/Mg^{2+} . 251 Slides were mounted with Prolong Gold anti-fade agent (Life Technologies). Images were 252 obtained using a spinning-disk confocal microscope (Quorum) with MetaMorph software and 253 were processed using ImageJ. For immunoblotting, cell lysate was extracted and 30µg of 254 protein was used per lane. Antibodies used are listed in Additional file 1: Table S1. 255

256 FACS analysis

For each experiment, approximately one million cells were pelleted, washed with PBS -257 Ca^{2+}/Mg^{2+} , resuspended in PBS – Ca^{2+}/Mg^{2+} and fixed by adding 70% ice-cold ethanol dropwise 258 while vortexing. Cells were stained with 10ug/mL propidium iodide (Sigma) and 200ug/mL 259 RNase A (Fisher Scientific) in FACS buffer (PBS – Ca²⁺/Mg²⁺, 0.2% BSA, 1mM EDTA). FACS 260 261 was performed on single-cell suspensions and the cell cycle analysis function of FlowJo was used to analyze cell cycle composition for each sample, based on propidium iodide staining to 262 263 detect DNA content in each cell. p-values: *P<0.05, **P<0.01, ***P<0.001 were determined by a two-tailed Student's t-test. 264

265 RNA-Seq and RT-qPCR

Total RNA was collected from iPSC-derived day 12 cExN and cIN NPCs using the NucleoSpin 266 267 RNA II kit (Takara) per the manufacturer's instructions. RNA was quantified using a NanoDrop ND-1000 spectrophotometer (Thermo Scientific), and the integrity of RNA was confirmed with 268 269 an Agilent Bioanalyzer 2100 to ensure a RIN value above eight. RNA-sequencing (RNA-seq) 270 library preparation and Illumina sequencing were performed by the Genome Technology Access Center at Washington University. For RT-gPCR, 1µg total RNA was reverse transcribed using 271 272 iScript Reverse Transcription Supermix (Bio-Rad). Equal guantities of cDNA were used as a template for RT-gPCR, using the Applied Biosystems Fast Real-Time guantitative PCR system. 273 RPL30 mRNA levels were used as endogenous controls for normalization. p-values: *P<0.05, 274 **P<0.01, ***P<0.001 were determined by a two-tailed Student's t-test. 275

276 Bioinformatics and IPA analyses

277 RNA-seq data analysis was performed as described in (33) to curate differentially expressed 278 gene (DEG) lists. To uncover the biological significance of DEGs, network analysis was 279 performed with the data interpretation tool Ingenuity Pathway Analysis (IPA) (Qiagen). IPA's 280 Ingenuity Knowledge Base uses network-eligible DEGs to generate networks and to define connections between one or more networks. Based on the number of eligible DEGs, IPA defines network scores as inversely proportional to the probability of finding the network and defines significant networks (p≤0.001). Within each network, red symbols indicate upregulated genes and green symbols indicate downregulated genes, where the color intensity represents relative degree of differential expression.

286 Results

287 Phenotyping and genotyping of the multiplex family

288 The multiplex Autism Spectrum Disorder (ASD) pedigree selected for study (Fig. 1; Table 1) underwent clinical phenotyping and genotyping (see Methods). From this pedigree, the 289 290 individuals selected for iPSC line derivation and modeling included the affected proband (AP), his sister, who has an intermediate phenotype (IS), and their unaffected mother (UM) (indicated 291 292 in Fig. 1). As described above, a non-synonymous single nucleotide variant in the GPD2 gene was identified in the UM and all of the children (chr2:157352686 (hg19) G>A, NM 001083112.2 293 c.233G>A, p.G78E). This variant is not present in the father. The variant is in exon three of the 294 GPD2 gene, within the region encoding the flavin adenine dinucleotide (FAD)-binding domain of 295 the GPD2 protein (Additional file 2: Fig. S1A). The GeneDx interpretation of this variant states 296 that it was not observed in approximately 6,500 individuals of European and African American 297 298 ancestry in the NHLBI Exome Sequencing Project and that it is evolutionarily conserved. In 299 addition, in silico analysis predicts that this variant is probably damaging to the protein structure 300 and function. Overall, GeneDx designated this as a variant of uncertain significance (VUS) 301 following the American College of Medical Genetics criteria. Subsequent mutation-specific testing and Sanger sequencing identified this same variant in the AP, IS and trait-affected 302 303 brother (TB), while absent in an unrelated, unaffected control (UC) (Additional file 2: Fig. S1B). 304 Given the differential affectation of members of this pedigree carrying this variant, it was

apparent that this inherited VUS was insufficient to cause ASD by itself, but may have
 contributed to polygenic risk/liability in this family.

307 Generation of subject-derived iPSC models and directed differentiation into cortical 308 excitatory neurons

309 Multiple clonal iPSC lines were derived from the UM, IS, and AP, and were characterized in 310 parallel with a single, clonal iPSC line derived from the UC. When grown in stem cell maintenance media, there were no observable differences in expression of pluripotency 311 markers between these iPSC lines, as assessed by RT-qPCR (Additional file 2: Fig. S1C) and 312 immunocytochemistry (ICC) (Additional file 2: Fig. S1D). In addition, no differences in GPD2 313 protein levels were detected in iPSCs by ICC (Additional file 2: Fig. S1D) or Western blotting 314 315 (Additional file 2: Fig. S1E). Finally, we used FACS analysis of propidium iodide (PI)-stained iPSCs to assess cell cycle progression and detected no observable differences between these 316 317 iPSC lines, which had similar percentages of cells in each stage of the cell cycle (Additional file 318 2: Fig. S1F-G).

319 In the cortex, as a result of their abnormal development, imbalances in glutamatergic excitatory neurons (cExN) and GABAergic inhibitory interneurons (cINs) are thought to 320 contribute to neurodevelopmental disorders including ASD (3, 5, 34). We therefore differentiated 321 iPSCs derived from the UC, and from three family members (the UM, IS and AP), in parallel into 322 either cExN or cIN neural progenitor cells (NPCs) and/or neurons, to determine if we observed 323 324 any alterations in the in vitro development of either or both of these neural cell types. We performed 12 days of cExN differentiation (four days as embryoid bodies (EBs) in V-bottom 325 plates, followed by eight days with the EBs plated for two-dimensional (2-D) culture; Fig. 2A). At 326 327 all time points assessed during this differentiation, the IS and AP lines generated significantly

328 smaller neurospheres than the UC and UM. The UM neurospheres were also slightly smaller329 than those of the UC (Fig. 2B-C).

330 To identify whether an increase in apoptosis and/or a decrease in proliferation could be 331 contributing to these differences in neurosphere size, we performed FACS analysis of PIstained cells at day four of differentiation and found that the IS and AP neurospheres had a 332 significantly higher fraction of sub-G1 (apoptotic) cells, compared to neurospheres derived from 333 the UM and UC lines (<2N DNA content; Fig. 2D-E, G). There was a corresponding decrease in 334 the percentage of cells in the G1 phase of the cell cycle in the IS and AP neurospheres (2N 335 336 DNA content; Fig. 2D, F-G). However, neurospheres from all lines had similar percentages of cells in the S and G2/M phases of the cell cycle, suggesting that their cell cycle characteristics 337 338 and rates of progression were otherwise similar (S phase and 4N DNA content; Fig. 2D, G). To 339 determine whether induction of neural differentiation was a stressor that was contributing to this increase in apoptosis in the IS and AP line-derived neurospheres, we compared sphere size 340 after culturing spheres from each line either in stem cell maintenance media (mTeSR) or in 341 342 neural induction media. In general, sphere size was larger for all cell lines when kept in mTeSR 343 media rather than neural induction media, while the differences in sphere size for the IS and AP versus the UC and UM was much less pronounced in mTeSR relative to differences seen under 344 neural induction conditions (Fig. 2H-I). These data suggest that, by comparison with the UC and 345 346 UM, the IS and AP lines have a slightly elevated propensity to undergo apoptosis upon 347 dissociation and sphere formation, while this is exacerbated by induction of neural differentiation. 348

We next maintained these four lines as NPCs after neural rosette selection at day 12 and then subjected them to PI staining and FACS analysis. Unlike the results from earlier time points, the cExN NPCs showed no significant differences in cell cycle across the four lines (Additional file 2: Fig. S2A-B), nor in the rate of growth/death over the course of culture for four

days (Additional file 2: Fig. S2C). However, morphological analysis by bright field imaging indicated a possible adhesion defect in the IS NPCs, as indicated by uneven growth on the cell culture plate surface (Additional file 2: Fig. S2D). At the NPC stage, GPD2 protein levels remained similar across the four lines, as was shown for iPSCs (Additional file 2: Fig. S2E).

357 Finally, to determine if the NPCs derived from the affected individuals exhibited an altered capacity to differentiate into cExN neurons, NPCs from the four lines were further 358 359 differentiated for 12 days as shown (Additional file 2: Fig. S3A) and subjected to ICC. No apparent differences between the four lines were observed in the expression of NPC markers 360 361 (PAX6, NESTIN, and SOX1) or markers of immature (TUJ1) and mature cExN neurons (VGLUT, MAP2) (Additional file 2: Fig. S3B). Furthermore, there were no observable differences 362 363 between the lines in the fraction of cells expressing Ki-67, a marker of cell proliferation, or 364 cleaved Caspase-3, a marker of apoptosis (Additional file 2: Fig. S3B).

365 Differentiation of subject-derived iPSCs into cortical interneuron progenitors

We also characterized cellular phenotypes of these four lines during differentiation into cIN NPCs, to determine any differences between the development of this neural cell type in lines derived from affected versus unaffected individuals. The differentiation scheme to produce cIN NPCs is outlined in Figure 3A. On day five of differentiation in this scheme, neurospheres derived from the IS line were smaller than those of the UM. Conversely, the AP line-derived neurospheres were slightly larger than the UM line neurospheres (Fig. 3B-C).

After dissociation on day 12 of differentiation, we assessed the cell cycle of the cIN NPCs using FACS of PI-stained cells. The IS and AP cIN NPCs had an increased sub-G1 cell population, compared to the UC and UM NPCs, an indication of increased apoptosis in the cells from the affected individuals (Fig. 3D). Correspondingly, there was a decrease in the proportion of cells in the G1 phase of the cell cycle (Fig. 3E-F). However, no differences were observed in

frequencies of cells in the S and G2 phases of the cell cycle between lines, suggesting that 377 these lines had similar proliferation rates (Additional file 2: Fig. S2F). This result was supported 378 by analysis of NPC cell counts after four days of growth, which revealed a significant reduction 379 380 in the number of AP NPCs, as well as a slight reduction in the number of IS NPCs, compared to 381 the UM NPCs (Additional file 2: Fig. S2G). These reductions in NPC number may result from the increased NPC apoptosis detected in our PI FACS analysis. The AP NPCs also exhibited 382 383 altered morphology that could indicate impaired adhesion capacity relative to the control UM/UC lines, which could also contribute to the reduction in the number of AP NPCs persisting in the 384 culture after four days of growth (Additional file 2: Fig. S2H). 385

Transcriptomic differences in neural progenitor cells derived from affected individuals versus controls

To investigate which classes of genes could be differentially expressed in neural cells from the 388 affected individuals, by comparison with the unaffected controls, we performed RNA-seq 389 390 analysis on both cExN and cIN NPCs at day 12 of differentiation for all four subject-derived lines. Four biological replicates were analyzed for each sample type and were clustered by 391 principal component analysis (PCA) of processed reads (Additional file 2: Fig. S4A-B). We 392 defined genes that were significantly differentially expressed genes (DEGs) in pairwise 393 394 comparisons of these four sample types for either cExN or cIN NPCs, selecting DEGs with a pvalue of <0.05 and a fold difference between sample types of >2 (Additional file 3: Table S2). In 395 a within-family comparison of the UM, IS, and AP samples, greater numbers of DEGs were 396 397 obtained in the cIN NPC pairwise comparisons, versus the numbers of DEGs obtained for cExN NPC pairwise comparisons (Additional file 2: Fig. S4C-D). These data indicate that the cIN 398 samples from the affected individuals (IS/AP) exhibit more transcriptomic differences from the 399 UM control than the affected individual-derived cExN samples. 400

401 We focused first on identifying classes of genes that were differentially expressed in 402 NPCs derived from the affected individuals, by comparison with unaffected controls. To do this, we defined the subset of DEGs that were similarly expressed in samples from both affected 403 404 individuals (AP/IS) but that differed in expression by comparison with the unaffected mother 405 (UM) sample. Relative expression is also shown for the UC, for a full cross-sample comparison. 452 and 437 DEGs for the cExN and cIN NPC samples met these criteria, respectively. 406 407 Hierarchical clustering and visualization of the relative expression of these DEGs across the four sample types is shown for the cExN NPCs (Fig. 4A, Additional file 4: Table S3). We next 408 409 used Ingenuity Pathway Analysis (IPA) to assess the potential biological significance of these genes. For the 452 DEGs in the cExN NPCs described above, the most significant function- and 410 disease-related gene ontology (GO) terms included 'behavior', 'neurological disease', and 411 412 'embryonic development' (Fig. 4B). Network analysis using IPA revealed several interesting networks of DEGs related to these GO terms, including networks related to 'locomotion' (from 413 414 DEGs within the 'behavior' GO term) and 'behavior and developmental disorder' (Fig. 4C-D). Within the 'locomotion' network, most genes were upregulated in the affected individuals 415 416 compared to the controls, including genes relating to neural adhesion and ion channels (Fig. 4C and Additional file 5: Table S4). Genes with known roles in NPCs or neurons, as well as stress-417 related genes were present in the larger 'behavior and developmental disorder' network (Fig. 4D 418 419 and Additional file 5: Table S4). Interestingly, another network comprising genes from the GO term 'neurological disease' is related to 'inflammation of central nervous system' (Additional file 420 2: Fig. S5A and Additional file 5: Table S4). 421

IPA analysis of the cIN DEGs also revealed several interesting classes of genes that were differentially expressed between the affected participants and unaffected control NPCderived samples. Hierarchical clustering and visualization of the relative expression of DEGs across the four sample types for the cIN NPCs is shown in Fig. 4E (Additional file 4: Table S3).

The top GO terms included 'developmental disorder', 'behavior', 'nervous system development 426 427 and function', 'psychological disorders', and 'neurological disease' (Fig. 4F). Within the term 'behavior', a network that includes 'learning', 'cognition', and 'behavior'-related genes was 428 429 identified (Fig. 4G, Additional file 5: Table S4). The network related to the GO term 430 'psychological disorder' includes genes related to 'anxiety disorders', 'mood disorders', and 'depressive disorder' (Fig. 4H). The 'nervous system development and function' network 431 432 includes genes involved in the 'quantity of neurons' and 'quantity of synapse', as well as cell 433 adhesion genes (Additional file 2: Fig. S5B and Additional file 5: Table S4). Finally, a 434 'neurological' network included a number of genes also present in the other networks (Additional file 2: Fig. S5C). Taken together, this analysis of DEGs in both cExN and cIN NPCs shows 435 evidence of altered expression of a number of neurological and psychological disease-relevant 436 437 gene classes in the AP- and IS-derived lines, relative to lines derived from the UM and/or UC.

438 Within-family comparison identifies a transcriptome signature specific to neural 439 progenitor cells derived from the ASD-affected proband

As differences in genetic background can confound differential gene expression analysis (35). 440 we also performed a pairwise, within-family data comparison of DEGs that distinguish the UM-, 441 IS-, and AP-derived samples, focusing on DEGs specific to the AP that could contribute to the 442 443 greater degree of affectation observed. Using pairwise comparisons of DEGs, we defined 190 genes which were uniquely differentially expressed in cExN NPCs from the AP (Fig. 5A). The 444 top GO terms associated with these AP-specific DEGs included 'psychological disorders', 445 'behavior', 'nervous system development and function', 'developmental disorder', and 446 447 'neurological disease' terms (Fig. 5B). Within the 'behavior' term, network analysis showed genes related to 'memory' and 'learning' to be dysregulated (Fig. 5C and Additional file 5: Table 448 S4). Within the 'nervous system development and function' term, a network of dysregulated 449 450 genes related to 'differentiation of neurons' was identified (Fig. 5D, Table S4).

Similar analysis was performed on the cIN samples, revealing 384 DEGs unique to the 451 AP samples in the within-family comparison (Fig. 5E). IPA analysis identified classes of DEGs 452 related to the GO terms 'psychological disorders', 'developmental disorder', 'neurological 453 454 disease', 'behavior', and 'nervous system development and function' (Fig. 5F). Within the 455 'behavior' disease term, a network of genes related to 'behavior' and 'cognition' was identified 456 (Fig. 5G and Additional file 5: Table S4). Within the 'nervous system development and function' 457 term, a network of genes related to 'development of neurons' and 'synaptic transmission' had 458 altered expression in the AP versus the IS/UM-derived samples (Fig. 5H and Additional file 5: 459 Table S4). Together, this analysis identifies AP-unique DEGs in both cExN and cIN NPCs, many of which are broadly related to neural development, as well as to specific aspects of ASD, 460 such as behavioral alterations. These gene expression changes therefore correlate with and 461 462 may contribute to, the severity of affectation in the AP.

463 Comparison of differentially expressed genes with ASD-associated genes and validation

464 The Simons Foundation Autism Research Initiative (SFARI) (36) maintains a database of genes that are mutated to cause, or contribute to, ASD risk. We compared our DEGs to these ASD 465 genes, to assess whether their dysregulated expression could contribute to affectation in these 466 individuals. Of 452 DEGs in the cExN differentiation scheme that had similar expression in the 467 468 AP and IS that differed from that seen in the UM, 30 (6.6%) were ASD genes (Fig. 6A). For the corresponding cIN NPC comparison, 46 of 437 DEGs (10.5%) were ASD genes in the SFARI 469 470 Gene database (Fig. 6B). Based upon the 1019 genes present in the SFARI Gene database 471 (36) and the total of 27,731 genes with >0.1 RPKM average expression across all cExN and cIN samples, the number of AP- and IS-specific DEGs that are AD genes is significantly greater 472 than would be expected by chance (hypergeometric distribution, $p=9.35 \times 10^{-5}$ and 1.95×10^{-12} for 473 cExN and cIN data, respectively). Therefore, it is possible that misregulated expression and 474

475 consequently function of ASD genes contributed to disruption of neural development and/or476 continues to contribute to altered neurological function in the IS and AP.

477 We validated the differential expression of a subset of the DEGs described above by RTgPCR analysis, isolating RNA from NPCs derived from a second set of iPSC clones that differed 478 from those used for the RNA-seq experiments. Expression changes of DEGs selected from the 479 cExN NPC RNA-seq data (Fig. 7A) were robustly recapitulated in these experiments (Fig. 7B). 480 481 Genes from the 'behavior and developmental disorder', from other identified networks, and genes involved in neurodevelopment were evaluated (Additional file 5: Table S4). We also 482 483 derived cIN NPC RNA from a second set of iPSC clones and validated the corresponding RNAseq data for a subset of the DEGs (Fig. 7C). Differential expression was assessed for SFARI 484 485 ASD genes (36), and for genes encoding transcription factors, ion channels, and cell adhesion 486 molecules (Fig. 7D-E and Additional file 5: Table S4). In addition, we validated a subset of DEGs in cINs which also had differential expression in cExN NPCs (Fig. 7E). Together, these 487 488 analyses revealed that, relative to unaffected individuals, samples from affected individuals 489 exhibited altered expression of classes of genes involved in behavior, learning, cognition, mood disorders, and neurodevelopment, including perturbed ASD gene expression, suggesting that 490 491 these differences could contribute to aberrant neural development or function in the affected individuals. 492

493 Discussion

In recent years, the genetic structure of Autism Spectrum Disorder (ASD) risk in the general population has been clarified. This work has confirmed that while, in some cases, deleterious, single gene variants are significant contributors to ASD, the vast proportion of population attributable risk is polygenic (2, 37). Furthermore, this risk is highly heritable, and individuals within a multiplex family typically exhibit variable degrees of affectation (31). Here, we modeled

499 cellular and molecular correlates of ASD within one such multiplex family, performing cortical 500 neural differentiation of iPSCs derived from several family members with differential affectation. In this family, both polygenic liability and a shared variant of unknown significance (VUS) may 501 502 contribute to risk. In cells derived from the affected individuals, we identified compromised 503 responses to differentiation cues and altered gene expression profiles during iPSC 504 differentiation into cortical excitatory (cExN) and inhibitory (cINs) neurons, compared to related 505 and unrelated unaffected controls. This work demonstrates that iPSC-based modeling can be 506 used to characterize these more genetically complex but prevalent forms of ASD, in addition to 507 modeling simplex and monogenic forms, which have been the focus of most studies to date. Moreover, these data provide information on physiologic and transcriptomic signatures of 508 multiplex autism, with which cellular models derived from other families and other combinations 509 510 of inherited susceptibility factors can be compared in future work.

Our phenotypic analysis of these four iPSC-based models of cortical neural development 511 512 included assays conducted in the stem cells, during neural specification, in the proliferating 513 NPCs, and during neuronal differentiation. During cExN NPC specification and during cIN NPC 514 propagation, models from both affected individuals exhibited elevated fractions of cells with sub-G1 DNA content, relative to control-derived models. These data suggest that models derived 515 from the affected individuals are less resistant to stressors, such as induction of differentiation, 516 517 with these stressors increasing the propensity for cells to undergo apoptosis. While the 518 molecular trigger for the induction of apoptosis here is unclear, expression of stress and apoptosis-related genes, such as CHCHD2, ANXA1, and SPATA18 are dysregulated in these 519 models (38-42). These findings are reminiscent of some observations made in prior work, in 520 521 which schizophrenia subject-derived iPSCs exhibited reduced neurosphere size (43) and 522 increased apoptosis was observed in Williams-Syndrome iPSC-derived NPCs (44). Interestingly, few studies report cellular alterations observed prior to the NPC stage, often 523

focusing predominantly on phenotypes seen in NPCs and mature neurons (7-19). While this may reflect a lack of earlier phenotypic changes in some models, our findings highlight the importance of tracking neurodevelopmental alterations from their earliest onset. A recent report underscores the value of using cellular modeling approaches that aim to recapitulate some aspects of *in vivo* neurodevelopment (20). This study found that direct conversion of iPSCs into neurons masked ASD-associated cellular phenotypes, which were observable during directed differentiation of iPSCs (20).

In our study, transcriptomic analysis of neural progenitor cells revealed dysregulated 531 expression in affected individuals compared to controls of gene networks related to behavior, 532 psychological disorders, and neuronal development and disease. Genes encoding transcription 533 534 factors were among the neurodevelopment-related genes with reduced expression in both 535 affected individuals. For example, ARX is required for normal telencephalic development and is 536 associated with syndromic autism and other neurodevelopmental disorders (45), while EMX1 and FOXB1 also play important roles in neural development (46-48). Behavioral misregulation is 537 538 a key trait of ASD, and gene networks related to the GO term 'behavior' exhibited dysregulated 539 expression in both affected individuals. Genes in these networks include COMT, ADCYAP1, 540 CNR1, HTR2C, GRIK2, and RGS4, all of which are implicated in behavior-related phenotypes in humans and/or mice (49-57). ASD genes were also dysregulated in these affected individuals, 541 542 relative to controls. Mutation of these genes in other individuals is implicated in autism risk or causation. These include adhesion-related genes (PCDHA1, PCHDHA6, PCDHGA11, PCDH8, 543 PCDH9, PCDH10 (58-62), KIRREL3 (63), CNTN3, CNTN4 (64), CNTNAP4 (65), and THBS1 544 (66)), receptor and channel genes (CACNA2D3 and SCN9A (67), GRIK2 and GRIK3 (68-71), 545 546 KCNJ2 (72, 73), and GRIA1 (74, 75)), and genes associated with central nervous system 547 development and axon guidance (ERBB4 (76, 77), NTNG1 (78), TSHZ3 (79), EBF3 (80), MYT1L (81, 82), and ANXA1 (40-42)). Altered expression of ASD-associated genes has also 548

been observed in cellular models derived from affected individuals in other studies (8, 13-16, 19,
83). Therefore, these findings suggest that misregulated expression of suites of ASD-associated
genes may contribute to risk or affectation, and may do so by altering neurodevelopment and/or
neuronal function in these affected individuals.

553 A unique aspect of this study is the use of iPSC-based directed differentiation into both cExNs and cINs, enabling us to identify neural cell type-specific alterations associated with 554 555 affectation. Although DEGs identified in affected individuals in both neural cell types were associated with many similar functions and diseases (e.g. behavior), the specific DEGs obtained 556 557 often varied by cell type. For example, cIN DEGs included many more ASD-associated genes and protocadherin genes, the latter of which control neuronal migration, axonal growth, and 558 559 synapse formation (60, 61). Human post-mortem cortical tissue from individuals with ASD has 560 been shown to exhibit disrupted expression of cIN-associated genes, evidence that this cell type 561 may commonly be disrupted in affected individuals in vivo (84). These findings suggest that extending cellular modeling studies to multiple disease-relevant neuronal cell types, including 562 563 cINs, may reveal additional neurodevelopmental disruptions related to affectation.

564 To define cellular and molecular perturbations commonly related to affectation, we compared our findings to other studies that modeled ASD by directed differentiation of iPSCs 565 566 into cExNs. We identified subsets of overlapping DEGs in comparisons with studies involving idiopathic autism cases vs. controls (26 shared DEGs; (7)), syndromic ASD involving 567 macrocephaly (31 shared DEGs; (19)), and modeling of the syndromic ASD gene CHD8 (32 568 569 shared DEGs; (13)) (Additional file 6: Table S5). Data for such comparisons is limited at present 570 because iPSC-based models have been generated for a relatively small number of individuals and mutations, and these almost exclusively characterize cExNs or cerebral organoids (7, 13, 571 18, 19). 572

573 The multiplex pedigree studied here was subjected to clinical exome sequencing, as it was 574 hypothesized that a single, shared, genetic contributor might mediate autism risk and differential phenotypic expression by sex in this family. In this sequencing analysis, a thread of shared 575 576 genetic liability amongst all children was a VUS in the ASD and ID-associated gene, GPD2 (85-577 87), which was inherited from their mother. However, there is variable ASD expressivity 578 amongst these individuals, ranging from absent, to intermediate, to severe. In addition, both 579 males and females in the pedigree are variably affected, indicating the presence of other 580 significant contributors to variation in severity of affectation within this family. This observation is 581 consistent with recent evidence that genetic liability for ASD is prevalently polygenic, and that, even in multiplex pedigrees where a significant monogenic contributor has been identified, 582 additional polygenic risk can contribute to affectation (37). Moreover, this multiplex family was 583 584 prototypic in reflecting the most severe form of affectation occurring in a male.

We hypothesized that it might be possible to identify graded cellular phenotypes that 585 586 correlated with the level of severity of phenotypic expression. In general, we instead observed 587 many cellular and molecular alterations that were shared by the cellular models derived from the 588 affected individuals, while not being observed in those derived from the unaffected individuals. However, we did define some proband-specific DEGs, not present in the less severely affected 589 sister, many of which relate to behavior and nervous system development. A subset of these 590 591 DEGs had graded expression, exhibiting intermediate expression levels in the intermediate 592 phenotype sister, between her unaffected mother and her severely affected brother. These 593 findings suggest that both the degree of dysregulation of expression and the number and 594 identity of DEGs within these networks may contribute to the level of affectation. While further 595 experimentation might reveal additional graded phenotypes, particularly in mature neurons, ex 596 vivo cellular modeling cannot recapitulate many aspects of fetal and post-natal

597 neurodevelopment that may have been perturbed to contribute to the graded affectation598 observed in these individuals.

599 This work highlights several considerations for ongoing scientific efforts to model this 600 complex but prevalent form of ASD in future studies. First, since the unique characteristics of 601 any multiplex pedigree present challenges for cellular modeling, it is important to control for sex and variation in affectation in subject and family selection, study design, and analysis. Related 602 603 to this point is the importance of modeling affected females in such studies. Most ASD cellular 604 modeling to date has been restricted to affected males (7-10, 13, 14, 16, 18, 19), given the 605 increased prevalence of ASD among males, and the fact that constraint to a single sex simplifies some modeling considerations. In particular, sex chromosome dosage effects do not 606 607 need to be accounted for in male cells, while female-derived iPSC models cannot currently 608 recapitulate the process of random X-chromosome inactivation that occurs in developing 609 somatic tissues, including the brain (88, 89). Interestingly, the transcriptomic differences that we 610 observed here were not driven by sex-linked gene expression: very few DEGs in any potential 611 pairwise sample comparison (whether between same or opposite sex models) were sex 612 chromosome-linked potential contributors to sex-biased gene expression in the human brain (90, 91). Therefore, this work supports the feasibility of identifying DEGs associated with 613 614 affectation by cellular model cross-comparisons, even when these models are derived from both 615 female and male subjects.

Another consideration for iPSC-based modeling of ASD is genetic background, which can be a confounding variable for cross-comparisons (35). In this pedigree, ASD risk was polygenic, such that it was not possible to engineer a correction of a single genome variant to create pairs of isogenic mutant versus wild-type iPSC lines with an identical genetic background for study. In such cases, modeling of first degree relatives may serve as the best control, and modeling of multiple related individuals with varying affectation provides additional opportunities

for identifying potential contributors to these differences in affectation. Including unrelated controls and performing comparisons with other studies can further highlight which phenotypic and transcriptomic alterations track with affectation, even by comparison with models derived from individuals with an unrelated genetic background.

626 Conclusions

627 In summary, this work used robust schemes for differentiation of cortical neurons from iPSCs to model cellular and molecular signatures associated with multiplex ASD in a family reflecting 628 629 varying degrees of affectation. Even in this prevalent, complex form of ASD, involving heritability, polygenic etiology, and variable affectation, we could identify affectation-linked 630 631 cellular and molecular alterations of neurodevelopment, some of which overlapped those defined in other iPSC-based studies of monogenic, syndromic, and de novo ASD. As more 632 cellular models of ASD are characterized, these data can be harnessed in the search for 633 634 convergent and divergent contributors to impairment across the genetically complex and multi-635 factorial pathways that give rise to ASD.

636 Abbreviations

- 637 ASD: Autism Spectrum Disorder; iPSCs: Induced Pluripotent Stem Cells; cExNs: Cortical
- 638 Excitatory Neurons; clNs: Cortical Inhibitory Neurons; NPCs: Neural Progenitor Cells; ES:
- 639 Exome Sequencing; UM: Unaffected Mother; AP: Affected Proband; IS: Intermediate Phenotype
- 640 Sister; UC: Unaffected Control; GTAC: Genome Technology Access Center; ICC:
- 641 Immunocytochemistry; RT-qPCR: quantitative reverse transcription PCR; EBs: Embryoid
- Bodies; DEG: Differentially Expressed Gene; IPA: Ingenuity Pathway Analysis; VUS: Variant of
- 643 Unknown Significance; PI: Propidium Iodide; PCA: Principal Component Analysis; GO: Gene
- 644 Ontology; SFARI: Simons Foundation Autism Research Initiative.

645 Ethics approval and consent to participate

- 646 Subjects were consented for biobanking and iPSC line generation by the Washington University
- 647 Institutional Review Board of the Human Research Protection Office under human studies
- 648 protocol #201409091 (Dr. John Constantino).

649 **Consent for publication**

650 Consent to publish data was provided by all subjects.

651 Availability of data and materials

- The RNA-seq data generated during the current study are available in the Gene Expression
- 653 Omnibus (GEO) repository as Series GSE129806. The ASD gene dataset analyzed during the
- 654 current study is available in the SFARI Gene database at https://gene.sfari.org.

655 Competing interests

The authors declare that they have no competing interests.

657 Funding

This project was supported by NIH/NICHD grant U54 HD087011 to JNC; NIH/NIGMS GM

- 659 66815, March of Dimes Grant 1-FY13-413, WUSM Institute for Clinical and Translational
- 660 Sciences (ICTS) grant JIT-NOA_619 (from NIH/NCATS UL 1TR002345 to ICTS), and a grant
- 661 from the McDonnell Center for Cellular and Molecular Neurobiology at WUSM to KLK;
- 662 NIH/NIGMS T32 GM 7067-43, the Precision Medicine Pathway at WUSM, and the Irving Biome
- 663 Graduate Student Fellowship at WUSM to EMAL; NIH K12 HL120002 to DB.

664 Author's contributions

E.M.A.L. contributed to the study design, carried out all cExN experimentation, analyzed data,
and prepared the manuscript. K.M. contributed to the study design, carried out all clN
experimentation, analyzed data and contributed to manuscript preparation. D.B. interpreted
clinical exome sequencing data and contributed to manuscript preparation. P.G. and B.Z.
performed RNA-seq data analysis. A.B. contributed to the study design. J.N.C. contributed to
the study design and manuscript preparation. K.L.K. contributed to the study design, data
analysis, and manuscript preparation. All authors read and approved the final manuscript.

672 Acknowledgments

We thank the family for providing biomaterials for use in this study. We thank the Genome 673 674 Engineering and iPSC Center (GEiC) at Washington University School of Medicine (WUSM) for deriving the iPSC lines used in this study. We thank the Alvin J. Siteman Cancer Center at 675 676 WUSM, for the use of the Siteman Flow Cytometry Core, which provided self-service Flow 677 Cytometry Analysis. The Siteman Cancer Center is supported in part by an NCI Cancer Center Support Grant #P30 CA091842. We thank the Genome Technology Access Center in the 678 Department of Genetics at WUSM for providing genomic sequencing services. The Center is 679 680 partially supported by NCI Cancer Center Support Grant #P30 CA91842 to the Siteman Cancer 681 Center and by ICTS/CTSA Grant# UL1 TR000448 from NIH/NCRR.

682 Figure Legends

Table 1. Selected clinical characteristics and mutational status of several individuals in the multiplex ASD pedigree.

Figure 1. Pedigree from which samples were derived for this study. *GPD2* mutational status (GPD2m: indicates mutational status) and degree of ASD affectation are indicated. Black shading corresponds to the affected proband (AP) and his twin brother, dark grey to the intermediate phenotype sister (IS), light grey to the trait-affected brother (TB), and white to unaffected family members, including the unaffected mother (UM). * indicates that renal epithelial cells from these individuals were used to derive multiple, clonal iPSC lines.

691 Figure 2. Characterization of iPSC lines during differentiation into cExN NPCs. (A) Differentiation scheme, including timeline and small molecules used. (B-C) iPSCs derived from 692 693 an unrelated, unaffected control (UC), as well as the UM, IS, and AP were differentiated for 12 694 days to generate cExN NPCs. Neurosphere size at several time points is shown in (B) and quantified in (C) (mean±SEM; scale bar = 500µm; n=12 biological replicates, encompassing two 695 different clonal lines from each subject, and one clonal line for the UC). (D-G) At day four of 696 differentiation, cells were stained with propidium iodide and FACS analysis of DNA content was 697 performed. (D) Representative FACS plots. In (E) <2N (sub-G1) and (F) 2N (G1) cells are 698 699 quantified, with values shown for each replicate. (G) shows mean values for all cell cycle stages 700 for each cell line (mean±SEM; n≥3 biological replicates for each subject, encompassing two 701 different clonal lines from each subject, and one clonal line for the UC). (H-I) iPSCs were 702 differentiated in either induction media or mTeSR stem cell media, and EB size was analyzed at day four of differentiation. Representative images are shown in (H) (scale bar = 500μ m), with 703 704 quantification in (I) (n=3 biological replicates from one clonal line for each subject). p-values:

*P<0.05, **P<0.01, ***P<0.001 were determined by a two-tailed Student's t-test and all other pairwise comparisons had a non-significant p-value (P≥0.05).

Figure 3. Characterization of iPSC lines during differentiation into cIN NPCs. (A) 707 708 Differentiation scheme, including timeline and small molecules used. (B-C) iPSCs were differentiated for 12 days to obtain cIN NPCs, with differences in neurosphere size shown in (B) 709 and quantified in (C) (mean±SEM; scale bar = 250µm; n=3 biological replicates from one clonal 710 711 line for each subject). (D-F) NPCs were stained with propidium iodide and analyzed by FACS 712 for DNA content. In D and E, respectively, <2N (sub-G1) and 2N (G1) cells were quantified, with 713 values shown for each replicate (n=3 biological replicates from one clonal line for each subject). (F) shows representative FACS plots. p-values: *P<0.05, **P<0.01, ***P<0.001 were 714 715 determined by a two-tailed Student's t-test and all other pairwise comparisons had a non-716 significant p-value ($P \ge 0.05$).

717 Figure 4. Transcriptomic analysis of genes with differential expression in affected 718 subject-derived NPCs, relative to unaffected controls. (A) Hierarchical clustering of RNAseg data from the cExN NPCs identified differentially expressed genes (DEGs) with shared 719 720 expression in the AP and IS that differed from that in the UM. Relative expression is also shown for the UC, for a full cross-sample comparison (p<0.05, fold-change >2; n=4 biological replicates 721 from one clonal line for each subject). (B-D) Ingenuity Pathway Analysis (IPA) of these cExN 722 723 NPC DEGs defined disease and function-associated gene ontology (GO) terms and identified gene networks associated with the (C) 'behavior' (D) and 'behavior and developmental disorder' 724 725 GO terms. (E) Hierarchical clustering of RNA-seq data for the cIN NPCs identified DEGs with shared expression in the AP and IS, that differed from that in the UM. Relative expression is 726 also shown for the UC, for a full cross-sample comparison (p<0.05, fold-change >2; n=4 727 biological replicates from one clonal line for each subject). (F-H) IPA analysis of these cIN NPC 728 729 DEGs defined (F) disease- and function-associated GO terms and identified gene networks associated with (G) 'behavior' and (H) 'psychological disorder'. Within each network, red
 symbols indicate upregulated genes and green symbols indicate downregulated genes, while
 color intensity indicates relative degree of differential expression.

733 Figure 5. Within-family analysis of transcriptomic signatures specific to the affected

proband-derived samples. (A) Venn diagram for the cExN NPCs, showing the DEGs from

pairwise comparisons of different samples, including numbers of overlapping DEGs. The blue

shaded portion of the Venn diagram indicates DEGs unique to the AP, not shared by the IS or

737 UM. (B-D) Ingenuity Pathway Analysis (IPA) of the AP-unique DEGs in cExN NPCs defined

class and function-associated GO terms (B) and identified gene networks associated with

'behavior' (C) and 'nervous system development and function' (D). (E-H) IPA analysis of the AP-

vunique DEGs in cIN NPCs determined (F) class and function-associated GO terms and

identified gene networks associated with (G) 'behavior' and (H) 'nervous system development

and function'. Within each network, red symbols indicate upregulated genes and green symbols

indicate downregulated genes, where the color intensity represents relative degree of differentialexpression.

Figure 6. Hierarchical clustering of DEGs that are also ASD genes in the SFARI autism gene database. (A) Relative gene expression for the cExN NPC samples. (B) Relative gene expression for the cIN NPC samples. Data from four biological replicates are shown for each sample type.

749 Figure 7. Validation of DEGs of interest identified from RNA-seq experiments by RT-

qPCR. Genes tested are related to behavior and developmental disorders, adhesion, and ion
channels. (A-B) Comparison of relative gene expression in cExN NPCs for the UM, IS, and AP
by (A) RNA-seq and (B) RT-qPCR, including expression analysis of genes related to 'behavior
and developmental disorders'. (C-E) Comparison of gene expression between the UM, IS and

- AP for the cIN NPCs by (C) RNA-seq and by (D-E) RT-qPCR, both for genes that were (D)
- differentially expressed only in the cIN NPCs and (E) for genes that were differentially
- expressed in both cExN and cIN NPCs. p-values: *P<0.05, **P<0.01, ***P<0.001 were
- 757 determined by a two-tailed Student's t-test and all other pairwise comparisons had a non-
- significant p-value ($P \ge 0.05$). RT-qPCR data shown includes n ≥ 3 biological replicates from one
- clonal line per subject, where samples were generated for each subject by using a second
- clonal iPSC line that differed from the line used for RNA-seq analysis.

761 Additional files

762	Additional	file	1:	Table	S1.	Antibodies	used	in	immunocytochemistry	and	immunoblotting
763	experiments	s (XL	.sx	.).							

764 Additional file 2: Figures S1-S5. Figure legends provided in file (PDF).

Additional file 3: Table S2. DEGs from pairwise comparisons of the four sample types for
 cExN or cIN NPCs (XLSX).

- 767 Additional file 4: Table S3. Hierarchical clustering of the relative expression of DEGs across
- the four sample types for cExN and cIN NPCs was performed using ClustVis. Order of genes in
- the cluster and unit variance scaled relative expression values are indicated (XLSX).
- 770 Additional file 5: Table S4. Details about selected DEGs within IPA networks (PDF).
- 771 Additional file 6: Table S5. cExN DEG comparison to other studies (XLSX).
- 772

773

- 774
- 775
- 776
- 777
- 778
- 779

780

782 References

- Wing L, Gould J. Severe impairments of social interaction and associated abnormalities
 in children: epidemiology and classification. J Autism Dev Disord. 1979;9(1):11-29.
- 2. Gaugler T, Klei L, Sanders SJ, Bodea CA, Goldberg AP, Lee AB, et al. Most genetic risk
- for autism resides with common variation. Nat Genet. 2014;46(8):881-5.
- 3. Donovan AP, Basson MA. The neuroanatomy of autism a developmental perspective. J
 Anat. 2017;230(1):4-15.
- 4. Ecker C, Bookheimer SY, Murphy DG. Neuroimaging in autism spectrum disorder: brain
 structure and function across the lifespan. Lancet Neurol. 2015;14(11):1121-34.
- 791 5. Zikopoulos B, Barbas H. Altered neural connectivity in excitatory and inhibitory cortical
 792 circuits in autism. Front Hum Neurosci. 2013;7:609.
- Canitano R, Pallagrosi M. Autism Spectrum Disorders and Schizophrenia Spectrum
 Disorders: Excitation/Inhibition Imbalance and Developmental Trajectories. Front Psychiatry.
 2017;8:69.
- 796 7. DeRosa BA, El Hokayem J, Artimovich E, Garcia-Serje C, Phillips AW, Van Booven D,
 797 et al. Convergent Pathways in Idiopathic Autism Revealed by Time Course Transcriptomic
 798 Analysis of Patient-Derived Neurons. Sci Rep. 2018;8(1):8423.
- Liu X, Campanac E, Cheung HH, Ziats MN, Canterel-Thouennon L, Raygada M, et al.
 Idiopathic Autism: Cellular and Molecular Phenotypes in Pluripotent Stem Cell-Derived Neurons.
 Mol Neurobiol. 2017;54(6):4507-23.
- 9. Aksoy I, Utami KH, Winata CL, Hillmer AM, Rouam SL, Briault S, et al. Personalized
 genome sequencing coupled with iPSC technology identifies GTDC1 as a gene involved in
 neurodevelopmental disorders. Hum Mol Genet. 2017;26(2):367-82.

805 10. Griesi-Oliveira K, Acab A, Gupta AR, Sunaga DY, Chailangkarn T, Nicol X, et al.
806 Modeling non-syndromic autism and the impact of TRPC6 disruption in human neurons. Mol
807 Psvchiatry. 2015;20(11):1350-65.

11. Deshpande A, Yadav S, Dao DQ, Wu ZY, Hokanson KC, Cahill MK, et al. Cellular
Phenotypes in Human iPSC-Derived Neurons from a Genetic Model of Autism Spectrum
Disorder. Cell Rep. 2017;21(10):2678-87.

12. Kathuria A, Nowosiad P, Jagasia R, Aigner S, Taylor RD, Andreae LC, et al. Stem cellderived neurons from autistic individuals with SHANK3 mutation show morphogenetic
abnormalities during early development. Mol Psychiatry. 2018;23(3):735-46.

13. Wang P, Lin M, Pedrosa E, Hrabovsky A, Zhang Z, Guo W, et al. CRISPR/Cas9mediated heterozygous knockout of the autism gene CHD8 and characterization of its transcriptional networks in neurodevelopment. Mol Autism. 2015;6:55.

Wang P, Mokhtari R, Pedrosa E, Kirschenbaum M, Bayrak C, Zheng D, et al.
CRISPR/Cas9-mediated heterozygous knockout of the autism gene CHD8 and characterization
of its transcriptional networks in cerebral organoids derived from iPS cells. Mol Autism.
2017;8:11.

15. Woodbury-Smith M, Deneault E, Yuen RKC, Walker S, Zarrei M, Pellecchia G, et al.
Mutations in RAB39B in individuals with intellectual disability, autism spectrum disorder, and
macrocephaly. Mol Autism. 2017;8:59.

16. Deneault E, White SH, Rodrigues DC, Ross PJ, Faheem M, Zaslavsky K, et al.
Complete Disruption of Autism-Susceptibility Genes by Gene Editing Predominantly Reduces
Functional Connectivity of Isogenic Human Neurons. Stem Cell Reports. 2018;11(5):1211-25.

Russo FB, Freitas BC, Pignatari GC, Fernandes IR, Sebat J, Muotri AR, et al. Modeling
the Interplay Between Neurons and Astrocytes in Autism Using Human Induced Pluripotent
Stem Cells. Biol Psychiatry. 2018;83(7):569-78.

18. Marchetto MC, Belinson H, Tian Y, Freitas BC, Fu C, Vadodaria K, et al. Altered
proliferation and networks in neural cells derived from idiopathic autistic individuals. Mol
Psychiatry. 2017;22(6):820-35.

19. Mariani J, Coppola G, Zhang P, Abyzov A, Provini L, Tomasini L, et al. FOXG1Dependent Dysregulation of GABA/Glutamate Neuron Differentiation in Autism Spectrum
Disorders. Cell. 2015;162(2):375-90.

Schafer ST, Paquola ACM, Stern S, Gosselin D, Ku M, Pena M, et al. Pathological
priming causes developmental gene network heterochronicity in autistic subject-derived
neurons. Nat Neurosci. 2019.

21. Christensen DL, Baio J, Van Naarden Braun K, Bilder D, Charles J, Constantino JN, et
al. Prevalence and Characteristics of Autism Spectrum Disorder Among Children Aged 8 Years
-Autism and Developmental Disabilities Monitoring Network, 11 Sites, United States, 2012.
MMWR Surveill Summ. 2016;65(3):1-23.

22. Constantino JN, Todorov A, Hilton C, Law P, Zhang Y, Molloy E, et al. Autism
recurrence in half siblings: strong support for genetic mechanisms of transmission in ASD.
Molecular psychiatry. 2013;18(2):137-8.

Gronborg TK, Schendel DE, Parner ET. Recurrence of autism spectrum disorders in fulland half-siblings and trends over time: a population-based cohort study. JAMA Pediatr.
2013;167(10):947-53.

24. Constantino JN. Recurrence rates in autism spectrum disorders. Jama.2014;312(11):1154-5.

25. Constantino JN, Zhang Y, Frazier T, Abbacchi AM, Law P. Sibling recurrence and the genetic epidemiology of autism. The American journal of psychiatry. 2010;167(11):1349-56.

26. Ozonoff S, Young GS, Carter A, Messinger D, Yirmiya N, Zwaigenbaum L, et al.
Recurrence risk for autism spectrum disorders: a Baby Siblings Research Consortium study.
Pediatrics. 2011;128(3):e488-95.

27. De Rubeis S, He X, Goldberg AP, Poultney CS, Samocha K, Cicek AE, et al. Synaptic,

transcriptional and chromatin genes disrupted in autism. Nature. 2014;515(7526):209-15.

858 28. Mefford HC, Batshaw ML, Hoffman EP. Genomics, intellectual disability, and autism. N
859 Engl J Med. 2012;366(8):733-43.

29. Turner TN, Eichler EE. The Role of De Novo Noncoding Regulatory Mutations in
Neurodevelopmental Disorders. Trends Neurosci. 2018.

30. Williams SM, An JY, Edson J, Watts M, Murigneux V, Whitehouse AJO, et al. An integrative analysis of non-coding regulatory DNA variations associated with autism spectrum disorder. Mol Psychiatry. 2018.

31. Griesi-Oliveira K, Sertie AL. Autism spectrum disorders: an updated guide for genetic
counseling. Einstein (Sao Paulo). 2017;15(2):233-8.

867 32. Retterer K, Juusola J, Cho MT, Vitazka P, Millan F, Gibellini F, et al. Clinical application
868 of whole-exome sequencing across clinical indications. Genet Med. 2016;18(7):696-704.

33. Meganathan K, Lewis EMA, Gontarz P, Liu S, Stanley EG, Elefanty AG, et al.
Regulatory networks specifying cortical interneurons from human embryonic stem cells reveal
roles for CHD2 in interneuron development. Proc Natl Acad Sci U S A. 2017;114(52):E11180E9.

873 34. Lunden JW, Durens M, Phillips AW, Nestor MW. Cortical interneuron function in autism
874 spectrum condition. Pediatr Res. 2019;85(2):146-54.

35. Hoekstra SD, Stringer S, Heine VM, Posthuma D. Genetically-Informed Patient Selection
for iPSC Studies of Complex Diseases May Aid in Reducing Cellular Heterogeneity. Front Cell
Neurosci. 2017;11:164.

878 36. SFARI gene Database. <u>https://www.sfari.org/resource/sfari-gene/</u>. Accessed December
879 2018.

Weiner DJ, Wigdor EM, Ripke S, Walters RK, Kosmicki JA, Grove J, et al. Polygenic
transmission disequilibrium confirms that common and rare variation act additively to create risk
for autism spectrum disorders. Nat Genet. 2017;49(7):978-85.

883 38. Wang DB, Kinoshita C, Kinoshita Y, Morrison RS. p53 and mitochondrial function in 884 neurons. Biochim Biophys Acta. 2014;1842(8):1186-97.

39. Liu Y, Clegg HV, Leslie PL, Di J, Tollini LA, He Y, et al. CHCHD2 inhibits apoptosis by
interacting with Bcl-x L to regulate Bax activation. Cell Death Differ. 2015;22(6):1035-46.

40. Solito E, McArthur S, Christian H, Gavins F, Buckingham JC, Gillies GE. Annexin A1 in the brain--undiscovered roles? Trends Pharmacol Sci. 2008;29(3):135-42.

41. Correia CT, Conceicao IC, Oliveira B, Coelho J, Sousa I, Sequeira AF, et al. Recurrent
duplications of the annexin A1 gene (ANXA1) in autism spectrum disorders. Mol Autism.
2014;5(1):28.

42. Parente L, Solito E. Annexin 1: more than an anti-phospholipase protein. Inflamm Res.
2004;53(4):125-32.

43. Toyoshima M, Akamatsu W, Okada Y, Ohnishi T, Balan S, Hisano Y, et al. Analysis of induced pluripotent stem cells carrying 22g11.2 deletion. Transl Psychiatry. 2016;6(11):e934.

44. Chailangkarn T, Trujillo CA, Freitas BC, Hrvoj-Mihic B, Herai RH, Yu DX, et al. A human
neurodevelopmental model for Williams syndrome. Nature. 2016;536(7616):338-43.

45. Friocourt G, Poirier K, Rakic S, Parnavelas JG, Chelly J. The role of ARX in cortical development. Eur J Neurosci. 2006;23(4):869-76.

46. Zhang Y, Hoxha E, Zhao T, Zhou X, Alvarez-Bolado G. Foxb1 Regulates Negatively the
Proliferation of Oligodendrocyte Progenitors. Front Neuroanat. 2017;11:53.

47. Takebayashi-Suzuki K, Kitayama A, Terasaka-lioka C, Ueno N, Suzuki A. The forkhead
transcription factor FoxB1 regulates the dorsal-ventral and anterior-posterior patterning of the
ectoderm during early Xenopus embryogenesis. Dev Biol. 2011;360(1):11-29.

48. Kobeissy FH, Hansen K, Neumann M, Fu S, Jin K, Liu J. Deciphering the Role of Emx1
in Neurogenesis: A Neuroproteomics Approach. Front Mol Neurosci. 2016;9:98.

49. Hattori S, Takao K, Tanda K, Toyama K, Shintani N, Baba A, et al. Comprehensive
behavioral analysis of pituitary adenylate cyclase-activating polypeptide (PACAP) knockout
mice. Front Behav Neurosci. 2012;6:58.

50. Shintani N, Hashimoto H, Tanaka K, Kawagishi N, Kawaguchi C, Hatanaka M, et al.
Serotonergic inhibition of intense jumping behavior in mice lacking PACAP (Adcyap1-/-). Ann N
Y Acad Sci. 2006;1070:545-9.

51. Gogos JA, Morgan M, Luine V, Santha M, Ogawa S, Pfaff D, et al. Catechol-Omethyltransferase-deficient mice exhibit sexually dimorphic changes in catecholamine levels
and behavior. Proc Natl Acad Sci U S A. 1998;95(17):9991-6.

916 52. Qayyum A, Zai CC, Hirata Y, Tiwari AK, Cheema S, Nowrouzi B, et al. The Role of the
917 Catechol-o-Methyltransferase (COMT) GeneVal158Met in Aggressive Behavior, a Review of
918 Genetic Studies. Curr Neuropharmacol. 2015;13(6):802-14.

53. Bowers ME, Ressler KJ. Sex-dependence of anxiety-like behavior in cannabinoid
receptor 1 (Cnr1) knockout mice. Behav Brain Res. 2016;300:65-9.

921 54. Paes LA, Torre OHD, Henriques TB, de Mello MP, Celeri E, Dalgalarrondo P, et al. 922 Association between serotonin 2C receptor gene (HTR2C) polymorphisms and 923 psychopathological symptoms in children and adolescents. Braz J Med Biol Res. 2018;51(8):e7252. 924

925 55. Martin CB, Ramond F, Farrington DT, Aguiar AS, Jr., Chevarin C, Berthiau AS, et al.
926 RNA splicing and editing modulation of 5-HT(2C) receptor function: relevance to anxiety and
927 aggression in VGV mice. Mol Psychiatry. 2013;18(6):656-65.

56. Shaltiel G, Maeng S, Malkesman O, Pearson B, Schloesser RJ, Tragon T, et al.
Evidence for the involvement of the kainate receptor subunit GluR6 (GRIK2) in mediating

930 behavioral displays related to behavioral symptoms of mania. Mol Psychiatry. 2008;13(9):858931 72.

57. Stratinaki M, Varidaki A, Mitsi V, Ghose S, Magida J, Dias C, et al. Regulator of G
protein signaling 4 [corrected] is a crucial modulator of antidepressant drug action in depression
and neuropathic pain models. Proc Natl Acad Sci U S A. 2013;110(20):8254-9.

935 58. Chen J, Yu S, Fu Y, Li X. Synaptic proteins and receptors defects in autism spectrum
936 disorders. Front Cell Neurosci. 2014;8:276.

937 59. Tsai NP, Huber KM. Protocadherins and the Social Brain. Biol Psychiatry.
938 2017;81(3):173-4.

939 60. Washbourne P, Dityatev A, Scheiffele P, Biederer T, Weiner JA, Christopherson KS, et
940 al. Cell adhesion molecules in synapse formation. J Neurosci. 2004;24(42):9244-9.

941 61. Wang X, Weiner JA, Levi S, Craig AM, Bradley A, Sanes JR. Gamma protocadherins
942 are required for survival of spinal interneurons. Neuron. 2002;36(5):843-54.

Bruining H, Matsui A, Oguro-Ando A, Kahn RS, Van't Spijker HM, Akkermans G, et al.
Genetic Mapping in Mice Reveals the Involvement of Pcdh9 in Long-Term Social and Object
Recognition and Sensorimotor Development. Biol Psychiatry. 2015;78(7):485-95.

63. Martin EA, Muralidhar S, Wang Z, Cervantes DC, Basu R, Taylor MR, et al. Correction:
The intellectual disability gene Kirrel3 regulates target-specific mossy fiber synapse
development in the hippocampus. Elife. 2016;5.

64. Mohebiany AN, Harroch S, Bouyain S. New insights into the roles of the contactin cell
adhesion molecules in neural development. Adv Neurobiol. 2014;8:165-94.

65. Karayannis T, Au E, Patel JC, Kruglikov I, Markx S, Delorme R, et al. Cntnap4
differentially contributes to GABAergic and dopaminergic synaptic transmission. Nature.
2014;511(7508):236-40.

954 66. Adams JC, Lawler J. The thrombospondins. Cold Spring Harb Perspect Biol. 955 2011;3(10):a009712.

956 67. Rubinstein M, Patowary A, Stanaway IB, McCord E, Nesbitt RR, Archer M, et al. 957 Association of rare missense variants in the second intracellular loop of NaV1.7 sodium 958 channels with familial autism. Mol Psychiatry. 2018;23(2):231-9.

- 959 68. Soto D, Altafaj X, Sindreu C, Bayes A. Glutamate receptor mutations in psychiatric and 960 neurodevelopmental disorders. Commun Integr Biol. 2014;7(1):e27887.
- 69. Contractor A, Mulle C, Swanson GT. Kainate receptors coming of age: milestones of two
 decades of research. Trends Neurosci. 2011;34(3):154-63.
- 70. Kim SA, Kim JH, Park M, Cho IH, Yoo HJ. Family-based association study between
 GRIK2 polymorphisms and autism spectrum disorders in the Korean trios. Neurosci Res.
 2007;58(3):332-5.
- 966 71. Pravetoni M, Wickman K. Behavioral characterization of mice lacking GIRK/Kir3 channel
 967 subunits. Genes Brain Behav. 2008;7(5):523-31.
- 968 72. Guglielmi L, Servettini I, Caramia M, Catacuzzeno L, Franciolini F, D'Adamo MC, et al.
 969 Update on the implication of potassium channels in autism: K(+) channelautism spectrum
 970 disorder. Front Cell Neurosci. 2015;9:34.
- 971 73. Binda A, Rivolta I, Villa C, Chisci E, Beghi M, Cornaggia CM, et al. A Novel KCNJ2
 972 Mutation Identified in an Autistic Proband Affects the Single Channel Properties of Kir2.1. Front
 973 Cell Neurosci. 2018;12:76.
- 74. Ramanathan S, Woodroffe A, Flodman PL, Mays LZ, Hanouni M, Modahl CB, et al. A
 case of autism with an interstitial deletion on 4q leading to hemizygosity for genes encoding for
 glutamine and glycine neurotransmitter receptor sub-units (AMPA 2, GLRA3, GLRB) and
 neuropeptide receptors NPY1R, NPY5R. BMC Med Genet. 2004;5:10.
- 978 75. Gu X, Zhou L, Lu W. An NMDA Receptor-Dependent Mechanism Underlies Inhibitory
 979 Synapse Development. Cell Rep. 2016;14(3):471-8.
- 980 76. Perez-Garcia CG. ErbB4 in Laminated Brain Structures: A Neurodevelopmental
 981 Approach to Schizophrenia. Front Cell Neurosci. 2015;9:472.

Yau HJ, Wang HF, Lai C, Liu FC. Neural development of the neuregulin receptor ErbB4
in the cerebral cortex and the hippocampus: preferential expression by interneurons tangentially
migrating from the ganglionic eminences. Cereb Cortex. 2003;13(3):252-64.

985 78. Yaguchi K, Nishimura-Akiyoshi S, Kuroki S, Onodera T, Itohara S. Identification of 986 transcriptional regulatory elements for Ntng1 and Ntng2 genes in mice. Mol Brain. 2014;7:19.

79. Caubit X, Gubellini P, Andrieux J, Roubertoux PL, Metwaly M, Jacq B, et al. TSHZ3
deletion causes an autism syndrome and defects in cortical projection neurons. Nat Genet.
2016;48(11):1359-69.

80. Sleven H, Welsh SJ, Yu J, Churchill MEA, Wright CF, Henderson A, et al. De Novo
Mutations in EBF3 Cause a Neurodevelopmental Syndrome. Am J Hum Genet.
2017;100(1):138-50.

81. Blanchet P, Bebin M, Bruet S, Cooper GM, Thompson ML, Duban-Bedu B, et al. MYT1L
mutations cause intellectual disability and variable obesity by dysregulating gene expression
and development of the neuroendocrine hypothalamus. PLoS Genet. 2017;13(8):e1006957.

82. Stevens SJ, van Ravenswaaij-Arts CM, Janssen JW, Klein Wassink-Ruiter JS, van
Essen AJ, Dijkhuizen T, et al. MYT1L is a candidate gene for intellectual disability in patients
with 2p25.3 (2pter) deletions. Am J Med Genet A. 2011;155A(11):2739-45.

999 83. Germain ND, Chen PF, Plocik AM, Glatt-Deeley H, Brown J, Fink JJ, et al. Gene 1000 expression analysis of human induced pluripotent stem cell-derived neurons carrying copy 1001 number variants of chromosome 15q11-q13.1. Mol Autism. 2014;5:44.

1002 84. Wang P, Zhao D, Lachman HM, Zheng D. Enriched expression of genes associated with
1003 autism spectrum disorders in human inhibitory neurons. Transl Psychiatry. 2018;8(1):13.

1004 85. Nguyen NH, Brathe A, Hassel B. Neuronal uptake and metabolism of glycerol and the 1005 neuronal expression of mitochondrial glycerol-3-phosphate dehydrogenase. J Neurochem. 1006 2003;85(4):831-42.

1007 86. Barge-Schaapveld DQ, Ofman R, Knegt AC, Alders M, Hohne W, Kemp S, et al.
1008 Intellectual disability and hemizygous GPD2 mutation. Am J Med Genet A. 2013;161A(5):10441009 50.

1010 87. Daoud H, Gruchy N, Constans JM, Moussaoui E, Saumureau S, Bayou N, et al. 1011 Haploinsufficiency of the GPD2 gene in a patient with nonsyndromic mental retardation. Hum 1012 Genet. 2009;124(6):649-58.

1013 88. Sahakyan A, Kim R, Chronis C, Sabri S, Bonora G, Theunissen TW, et al. Human Naive
1014 Pluripotent Stem Cells Model X Chromosome Dampening and X Inactivation. Cell Stem Cell.
1015 2017;20(1):87-101.

1016 89. Dandulakis MG, Meganathan K, Kroll KL, Bonni A, Constantino JN. Complexities of X 1017 chromosome inactivation status in female human induced pluripotent stem cells-a brief review 1018 and scientific update for autism research. J Neurodev Disord. 2016;8:22.

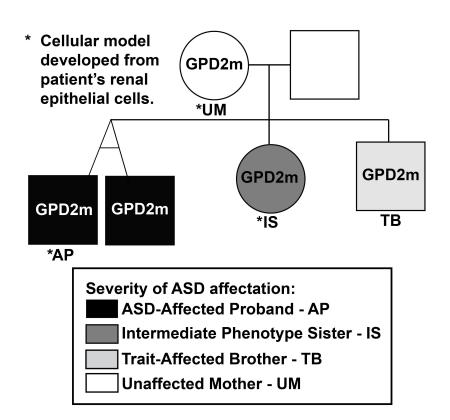
1019 90. Tukiainen T, Villani AC, Yen A, Rivas MA, Marshall JL, Satija R, et al. Landscape of X
1020 chromosome inactivation across human tissues. Nature. 2017;550(7675):244-8.

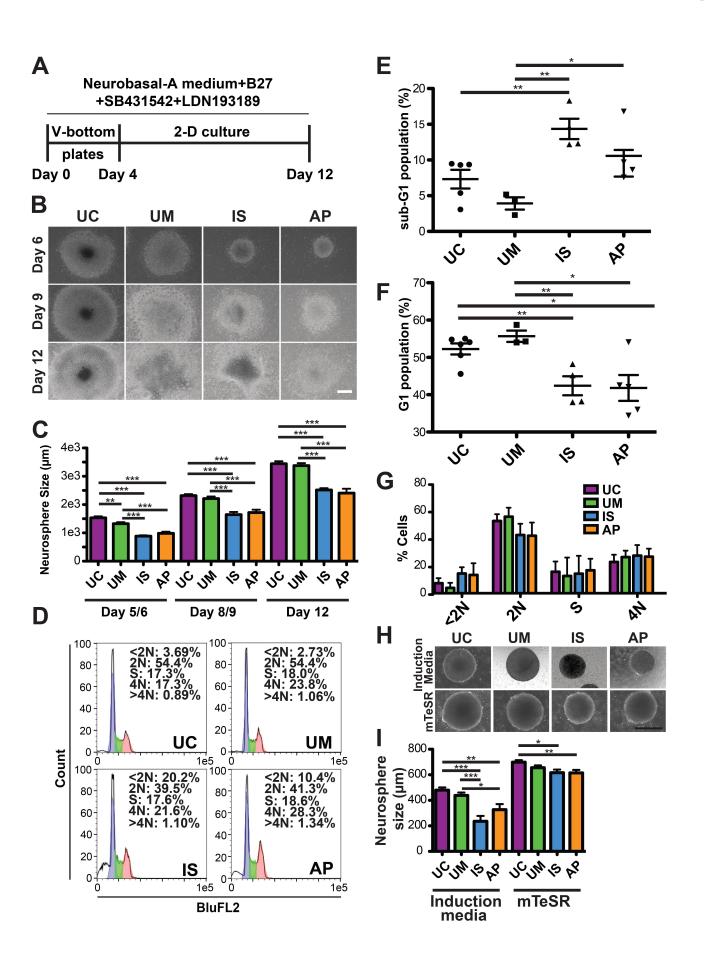
1021 91. Gershoni M, Pietrokovski S. The landscape of sex-differential transcriptome and its 1022 consequent selection in human adults. BMC Biol. 2017;15(1):7.

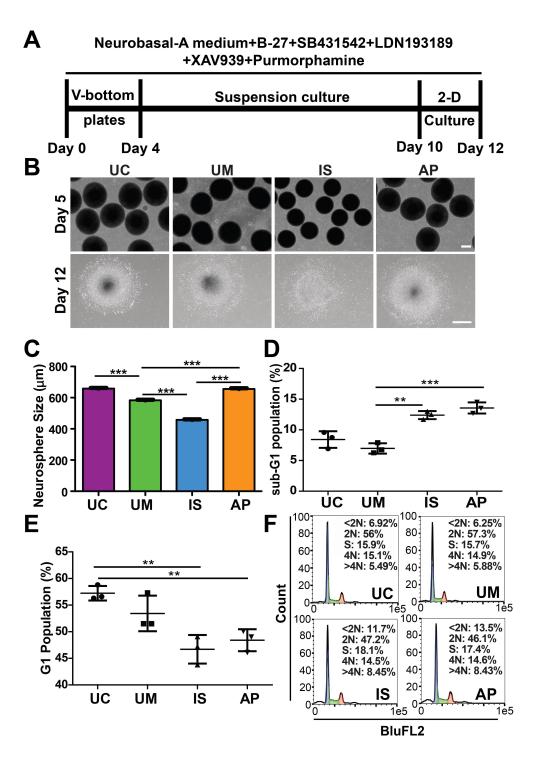
Table 1

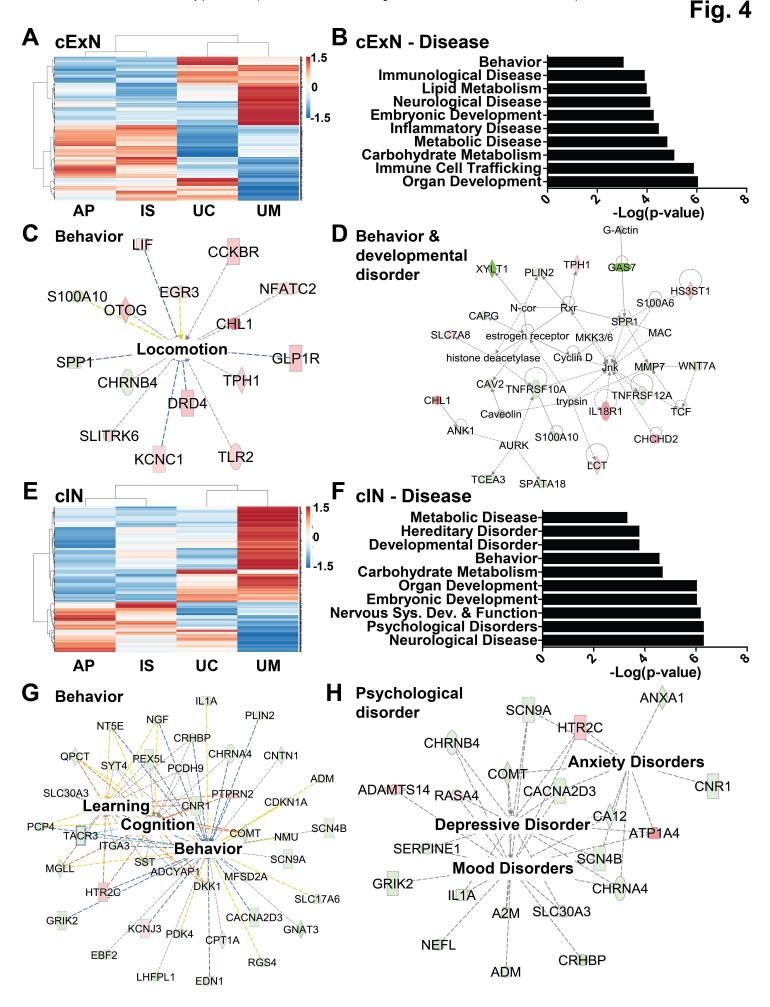
Clinical characteristic	AP	IS	UM
Age of ASD diagnostic confirmation	3.5 years	18 years	N/A
Social Responsiveness Scale-2	83T	72T	56T (spouse-report)
Depression and Anxiety	Yes	Yes	No
Seizure history	No	No	No
Developmental delay	Yes	No	No
Eye contact	Poor	Fair	Good
Repetitive behavior	Yes	No	No
Abnormal sensory sensitivities	Yes	No	No
IQ	65	102 (Raven)	108 (Raven)
Speech delay	Yes	No	No
ASD	Severe	Moderate	No
Intellectual Disability	Yes	No	No
	GPD2	GPD2	GPD2
Mutation location	chr2:157352686 (hg19) G>A	chr2:157352686 (hg19) G>A	chr2:157352686 (hg19) G>A
	p.G78E, c.233G>A	p.G78E, c.233G>A	p.G78E, c.233G>A

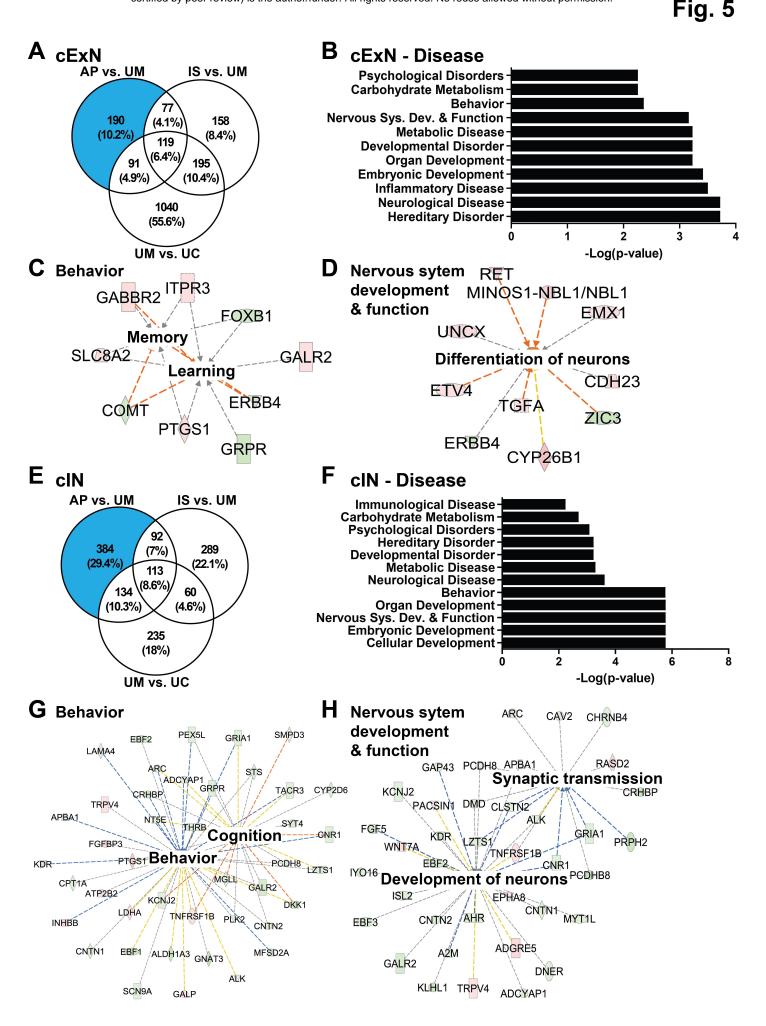
Fig. 1











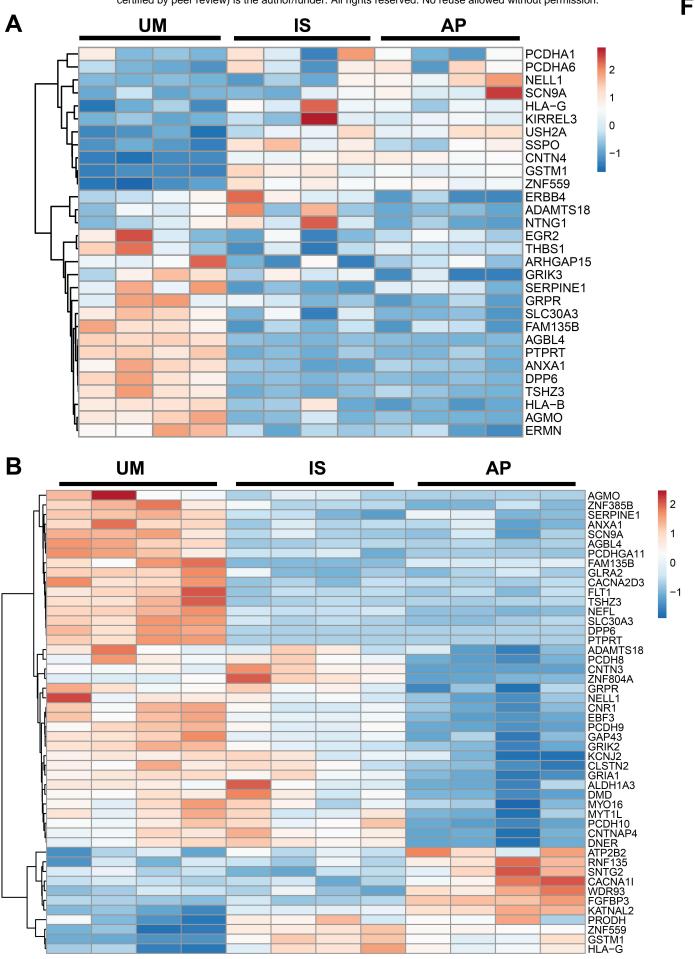


Fig. 6



